Journal of Thermal Analysis (1985) 901–911

COMPARATIVE ANALYSIS OF PURITY DETERMINATION METHODS USING A DIFFERENTIAL SCANNING CALORIMETER

A. A. Raskin

MENDELEEV ALL-UNION RESEARCH INSTITUTE OF METROLOGY, LENINGRAD, U.S.S.R.

(Received January 20, 1985)

Comparative analysis of several methods for purity determination using DSC is presented. This is based on a mathematical model including the construction of theoretical melting curves for two-component systems and the calculation of recorded melting curves with the help of a set of equations describing the formation of a DSC output signal. It is shown that the true accuracy of purity determinations in the range of impurity concentrations $\bar{x} = 0.005$–0.02 does not exceed 30–50%.

Purity determination is a very valuable and important application of DSC that has been subject of several reviews [2], [6–10], but the problem of establishing the true accuracy of DSC purity determinations has not yet been solved. This was convincingly demonstrated in [7] and [8], where it was shown that the relevant publications include obviously overstated estimates of accuracy as well as recommendations to apply DSC only for determination of the order of the impurity concentration.

The essence of the problem may be formulated as follows: for an isobaric melting process of a two-component eutectic system in thermodynamic equilibrium, function $T = f\left(\frac{1}{F}\right)$, where F is the fraction of the liquid phase in the system at temperature T, should be a straight line with slope proportional to the impurity concentration and cutting off the value of the melting temperature of the pure main component on the ordinate. However, functions $T = f\left(\frac{1}{F}\right)$ constructed on the basis of the experimental melting curves obtained with DSC turn out to be essentially nonlinear. The absence of thermodynamic equilibrium in a dynamic experiment, the inability of DSC to register the initial stages of melting, the formation of a solid solution, and the influence of thermal gradients, have all been indicated as possible causes of this nonlinearity. In order to eliminate the

John Wiley & Sons, Limited, Chichester
Akadémiai Kiadó, Budapest

nonlinearity, several methods have been proposed, the most widely known among them being those put forward by Sondack [1], Driscoll et al. [4] and Marti [2]. However, the results of purity determinations by any of these methods are strongly dependent on the portion of the $T = f\left(\frac{1}{F}\right)$ curve chosen for calculations, and for methods [2] and [4], which are iterative algorithms using the techniques of linear regression analysis, the results are also dependent on the iterative process parameters. Attempts to test the correctness of these methods and to establish the rules for data selection for calculations by applying these methods to specially prepared samples were not successful and led to the discrepancy pointed out in [7] and [8]. This is easily explained if account is taken of the fact that it is practically impossible to make samples of the required high purity with reliably known impurity concentration; this has repeatedly been pointed out, for example in [10]. Hence, it is worthwhile to carry out a theoretical comparative analysis of purity determination methods based on mathematical modelling of melting processes of two-component systems, taking into account the characteristic features of recording sharp endotherms by DSC.

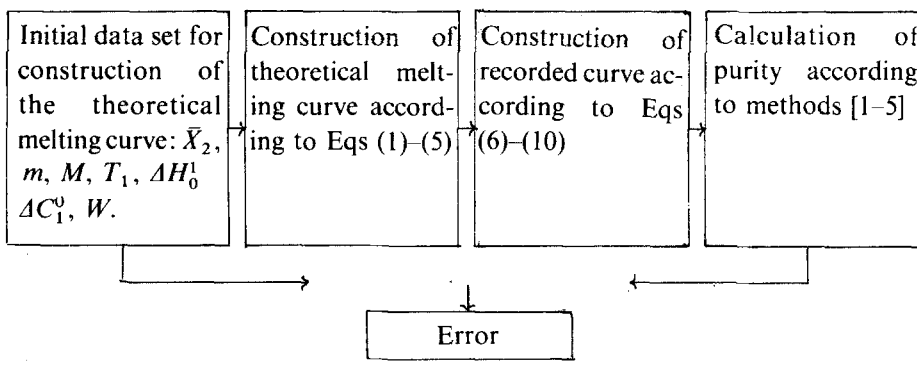

Fig. 1 Block diagram for comparative analysis

The procedure for such a comparative analysis, presented in Fig. 1, comprises the following stages:

1) construction of a theoretical melting curve;

2) construction of a mathematical model describing distortions of the theoretical melting curves during the recording of melting by DSC;

3) a numerical experiment in which a theoretical melting curve is constructed on the basis of the initial data set characterizing a two-component system; the curve recorded by DSC, when the melting process described by the theoretical melting curve has taken place in the DSC cell, is then constructed on the basis of the

mathematical model of the DSC; and this DSC-recorded curve is treated in accordance with the methods under consideration in order to obtain the calculated purity. Correlation of these calculated purity values with the initial values taken to plot the theoretical melting curve provides an opportunity for estimating the accuracy of these methods.

We use the results presented in [8], where the pertinent relations are derived and the algorithm for calculating the thermal power absorbed by the melting sample *vs.* the sample temperature is given, to plot the theoretical melting curve. From the well-known relation describing the isobaric melting process of a two-component eutectic system in equilibrium:

$$\frac{\Delta H_1}{RT^2}\,\mathrm{d}T = \mathrm{d}\ln(f_1 X_1) \tag{1}$$

taking into account the dependence of the main component melting enthalpy on temperature:

$$\Delta H_1 = \Delta H_1^0 + \Delta C_1^0 (T - T_1) \tag{2}$$

and the dependence of the activity coefficient of the main component on temperature and concentration in the form:

$$f_1 = l^{WX_2^2/RT} \tag{3}$$

the equation describing the phase diagram of a two-component eutectic system is derived in [8] in the form

$$\frac{\Delta H_1^0 + \Delta C_1^0 (T - T_1) + WX_2^2}{RT^2}\,\mathrm{d}T = \left(\frac{2WX_1}{RT} - \frac{1}{1 - X_2}\right)\mathrm{d}x_2;\ x_2 = \bar{x}/F \tag{4}$$

The algorithm presented in [8] allows calculation via (4) of the thermal power $\mathrm{d}H$ absorbed by one mole of the melting sample when its temperature changes at thermodynamic equilibrium from T to $T + \mathrm{d}T$. Consequently, in the dynamic mode the power $g_S(\tau)$ absorbed by the melting sample at the moment τ when the sample temperature equals $T(\tau)$ is expressed as

$$g_S[T(\tau)] = \frac{\mathrm{d}H}{\mathrm{d}T} \cdot \frac{\mathrm{d}T}{\mathrm{d}\tau} \cdot \frac{m}{M} \tag{5}$$

Equation (5) is the required theoretical melting curve, i.e. the power absorbed by the melting sample as a function of the sample temperature and the rate of its change. Notations in Eqs (1)–(5) are identical with those used in [8], i.e.

R = universal gas constant;

T = equilibrium temperature of the system;

i = 1, 2 = index relating to the main component and to the impurity, respectively;
T_i = melting temperature of the i-th pure component;
ΔH_i^0 = melting enthalpy of the i-th pure component;
ΔC_i^0 = difference between molar heat capacities in the solid and liquid phases of the i-th pure component;
x_i = molar fraction of the i-th component in the liquid phase;
$\bar{x}_i$ = total molar fraction of the i-th component in the system;
f_i = activity coefficient of the i-th component;
F = molten fraction at temperature T;
W = interaction energy between the components;
M = molecular weight.

Theoretical melting curves for a sample with $m = 2 \cdot 10^{-6}$ kg heated at a rate of 1 deg/min for various values of purity are presented in Fig. 2. The data set for the

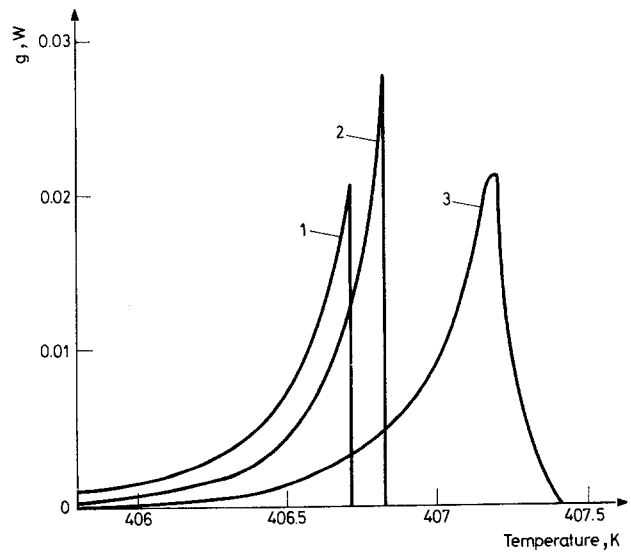

Fig. 2 Theoretical and recorded melting curves. (1) and (2) — Theoretical melting curves of $\bar{X}_2 = 0.007$ and $\bar{X}_2 = 0.005$, respectively; (3) — recorded melting curve for $\bar{X}_2 = 0.005$. Sample weight $m = 2.0$ mg; scanning rate $B = 1$ deg/min; thermal resistance $R_S = 80$ K/W

well-studied phenacetine-benzamide system from [8] was used for construction of the melting curve:

$\Delta H_1^0 = 32300$ J/mol; $\Delta C_1^0 = 55$ J/(mol·K); $W = 400$ J/mol; $T_1 = 407$ K; $M =$ 179,000 kg/mol.

The recordings of the thermal processes taking place in the DSC cell is always accompanied by distortions due to thermal resistances and lags in the differential power control loops. Let us establish the relationship between the power recorded by DSC and that absorbed by the sample, using the approach suggested in [14] for the DSM–2M calorimeter.

The design of the DSM–2M calorimeter block is based on a system of two identical cells controlled by two automatic control loops: the average power automatic control loop (ACL 1) and the differential power control loop (ACL 2), which is represented schematically in Fig. 3. The main features of the calorimeter performance essential for formulating the mathematical model of its operation are as follows. The average power automatic control loop supplies to both cells the reference power necessary for linear heating of the cells at the required rate of temperature change b. In doing so, ACL 1 continuously compares the reference cell temperature with the current value of the programmed temperature set by the temperature programmer. If there is a temperature difference between the programmed temperature T_p and the reference cell temperature, ACL 1 supplies

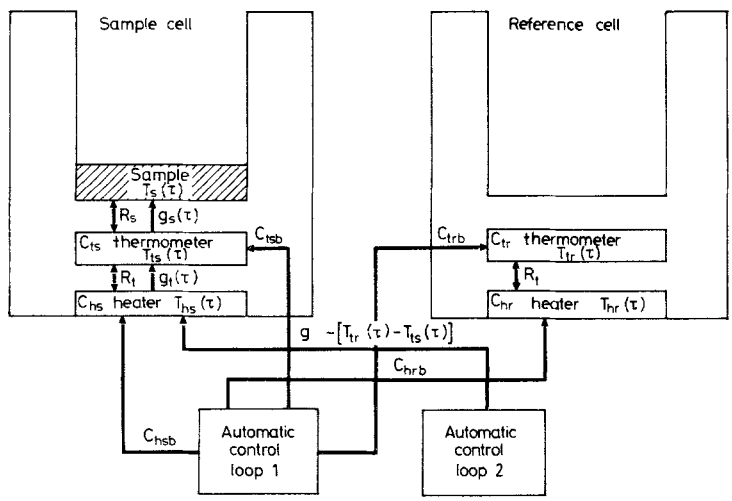

Fig. 3 Calorimetric block model

additional thermal power to the average power circuit in order to compensate for this temperature difference. As a result, the temperature of the reference cell, and those of its thermometer and heater, vary strictly at the required rate b, i.e. in accordance with the linear programme. It follows that thermal powers $C_{tr}b$ and $C_{hr}b$ are supplied to the thermometer and heater in the reference cell, respectively, from the average power circuit. Here C_{tr} and C_{hr} denote the heat capacities of the thermometer and heater of the reference cell. Just the same power as is supplied at

each instant of time to the reference cell is also fed to the sample cell. Since the cells are identical ($C_{hr} = C_{hS}$, $C_{tr} = C_{tS}$) but for the presence of the sample in the sample cell, we may assume that the same powers $C_{tS}b$ and $C_{hS}b$ are supplied to the sample cell thermometer and heater from the average power circuit when scanned at the rate b.

However, the thermal power absorbed by the melting sample cell from the sample cell bottom where the sample thermometer is positioned is large enough to distort the linear heating of the sample thermometer. As a result, the sample thermometer temperature begins to lag behind the reference cell thermometer temperature, which is maintained equal to the programmed temperature T_p with the help of ACL 1.

ACL 2 measures the temperature difference between the thermometers in the two cells and supplied additional power in accordance with the proportional-plus-integral control action to the sample cell in order to compensate for the temperature difference. This compensating power is recorded as a valid signal. Proceeding from the above, the thermal power balance for the sample cell thermometer and heater is

$$\begin{aligned} C_{tS}\frac{dT_{tS}}{d\tau} &= C_{tS}b + g_t(\tau) - g_S[T_S(\tau)] \\ C_{hS}\frac{dT_{hS}}{d\tau} &= C_{hS}b - g_t(\tau) + g^{rec}_{(\tau)} \end{aligned} \tag{6}$$

Here $T_S(\tau)$ = sample temperature at time τ, C_{tS} and C_{hS} = heat capacities of the sample thermometer and the sample heater; $g_t(\tau)$ = power supplied at moment τ from the sample heater to the sample thermometer through the contact thermal resistance (CTR) R_{tS}; $g_S[T_S(\tau)]$ = power supplied at moment τ for melting the sample at temperature $T_S(\tau)$; $g^{rec}_{(\tau)}$ = recorded power supplied to the sample heater from the differential power control loop; and τ = time. $g^{rec}_{(\tau)}$ is related to the temperature difference between the sample and reference thermometers by the relationship:

$$\begin{aligned} g^{rec}_{(\tau)} &= K_1[T_{tr}(\tau) - T_{tS}(\tau)] + K_2\int_0^{\tau}[T_{tr}(\Theta) - T_{tS}(\Theta)]d\Theta = \\ &= K_1[T_p(\tau) - T_{tS}(\tau)] + K_2\int_0^{\tau}[T_p(\Theta) - T_{ts}(\Theta)]d\Theta \end{aligned} \tag{7}$$

Here T_{tr} = reference cell thermometer temperature; T_{tS} = sample cell thermometer temperature at time τ; K_1 and K_2 = control action coefficients for ACL 2. In (7), account is taken of the fact that, as pointed out above, the following conditions are met

$$T_{tr}(\tau) = T_p(\tau); \quad \frac{dT_{tr}}{d\tau} = \frac{dT_p}{d\tau} = b \tag{8}$$

Let us take into account the existence of contact thermal resistances:

R_{tS} = CTR between the thermometer and the heater in the sample cell; R_S = overall CTR between the sample cell thermometer and the sample, including the thermal resistances of the sample-container and container-cell interfaces. The relationships between temperatures T_{tS} and T_{hS} then become

$$T_{tS}(\tau) = T_{hS}(\tau) - R_{tS}g_t(\tau)$$
$$T_{tS}(\tau) = T_S(\tau) - R_S g_S[T_S(\tau)] \tag{9}$$

Let us add the initial conditions to the set of Eqs (6)–(9):

$$T_{ts}(0) = T_{hs}(0) = T_p(0) = T_i \tag{10}$$

where t_i = programmed temperature at the instant of time $\tau = 0$, corresponding to the start of melting and taken to be zero moment, i.e. at $\tau > 0$ $T_p(\tau) = T_i + b\tau$.

It will be seen that numerical solution of a set of Eqs (6)–(10) enables one to calculate the function $g^{rec}[T_p(\tau)]$, which represents the DSC curve recorded for the sample melting in the DSC sample cell described by the theoretical melting curve, provided that this curve plotted according to Eqs (1)–(5) is used as $g_S[T_S(\tau)]$.

Values of C_{tS}, C_{hS}, K_1 and K_2 necessary for such calculations were determined using the relevant geometrical and thermophysical parameters of the sample and reference cells and the parameters of ACL 2 for the DSM–2M. Heat capacities were calculated as the sum of their associated members, and thermal resistances according to formulae recommended in [15]. Finally, the following values were used in calculations:

$$C_{ts} = 0.11 \text{ J/deg}: \; C_{hs} = 0.33 \text{ J/deg}; \; K_1 = 0.11 \text{ W/deg};$$
$$K_2 = 0.14 \cdot 10^{-3} \text{ W/(deg} \cdot \text{s)}; \; R_{ts} = 60 \text{ deg/W}.$$

Values of R_S characteristic of low molecular weight organic compounds were determined by the method recommended in [12] and [13], which is based on the relationship between the melting peak temperatures and the values of b and R_S. Values of R_S = 80–140 deg/W were used for calculations.

All calculations were incorporated in a FORTRAN programme for an ES–1033 computer. The programme was used to construct the theoretical melting curve on the basis of the initial data set, including values m, M, ΔH_1^0, ΔC_1^0, X_2, T_1 and W, to calculate the recorded melting curve for given values of b and R_S, to plot the $T = f\left(\frac{1}{F}\right)$ function for the recorded curve, and then to treat it in accordance with the methods proposed by Sondack [1], Marti [2], Cooksey and Hill [3], Driscoll et al. [4] and Gustin [5].

The $T = f\left(\frac{1}{F}\right)$ function for different values of b, R_S and m are presented in Fig. 4. It is obvious that during the DSC recording of melting there occur substantial distortions which cause a marked curvature of the $T = f\left(\frac{1}{F}\right)$ function, and that these distortions increase considerably with b, R_S and m. The results of comparative analysis of the above-mentioned methods for a set of parameters recommended in [7] as optimum values for purity determinations are presented in Fig. 5.

Analysis of Sondack's method, which gives the simplest means (using three points $i = 1, 2, 3$) of finding the average slope of the function $T = f\left(\frac{1}{F}\right)$, showed that determination of $\bar{X}_2$ with satisfactory accuracy is possible only if the values of $\frac{1}{F_i}$ ($i = 1, 2, 3$) prove to be chosen correctly, whereas recommendations for the choice of $\frac{1}{F_i}$ from [1] and [11] may lead to considerable errors. In principle, it is always possible to specify values of $\frac{1}{F_i}$ which ensure accurate calculations of $\bar{X}_2$, but these $\frac{1}{F_i}$ turn out to be strongly dependent on the impurity concentration that we are seeking and which is not known beforehand.

For example, for the phenacetine-benzamide system at $b = 1$ deg/min, $m = 2 \cdot 10^{-6}$ kg, $R_S = 100$ deg/W, these relationships take the form:

$$\begin{aligned} \frac{1}{F_1} &= 21.4 - 2732.1\bar{X}_2 + 110{,}985.9\bar{X}_2^2 \\ \frac{1}{F_2} &= 23.1 - 2936.5\bar{X}_2 + 118{,}796.8\bar{X}_2^2 \\ \frac{1}{F_3} &= 24.8 - 3154.8\bar{X}_2 + 121{,}552.5\bar{X}_2^2 \end{aligned} \tag{11}$$

As a result, it turns out to be impossible to preset values of $\frac{1}{F_i}$ which would ensure purity determinations with sufficient accuracy.

Somewhat better results may be achieved using the method [4] of Driscoll et al. and its more elaborate version (Marti), which formalizes the search for the initial portion of the curve $T = f\left(\frac{1}{F}\right)$ to be used in calculations.

In contrast to methods [1] (Sondack) and [3] (Cooksey and Hill), which yield only one value of the impurity concentration, methods [2] and [4] involve the

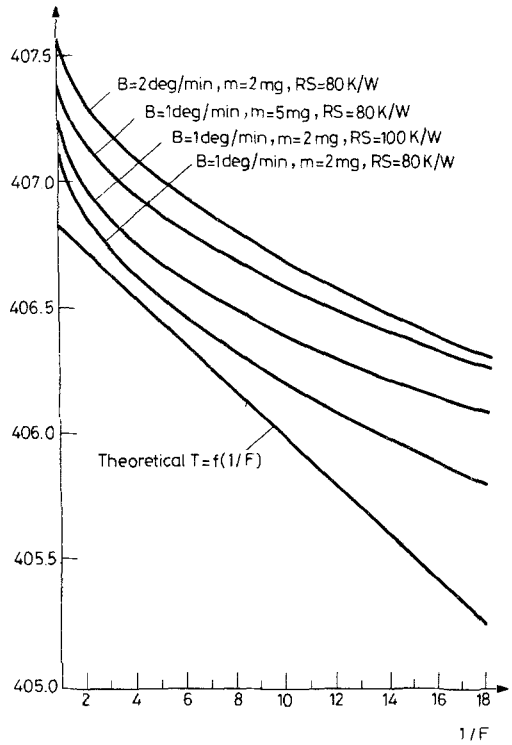

Fig. 4 Temperature *vs.* $1/F$ functions for different values of B, m, R_S

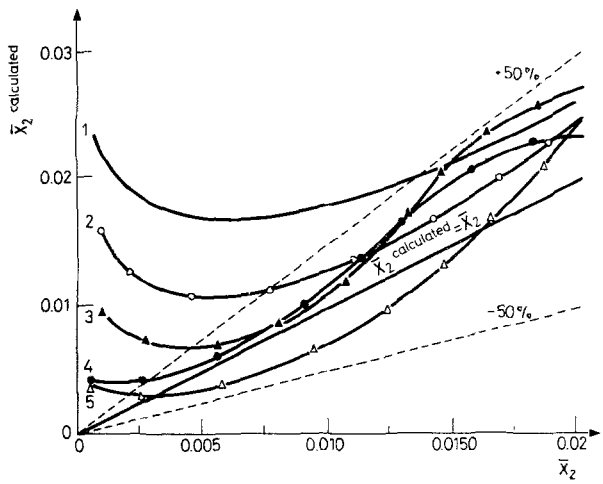

Fig. 5 Comparison of purity determination methods. (1) — Sondack [1]; (2) — Marti [2]; (3) — Cooksey and Hill [3]; (4) — Driscoll et al. [4]; (5) — Gustin [5]

construction of successive linear approximations of the curve $T = f\left(\frac{1}{F}\right)$ that produce a discrete spectrum of impurity concentrations with a 3–5% step over the range from obviously underestimated values of $\bar{X}_2$ to overestimated ones. Once again the efficiency of choosing the best linear approximation of the curve $T = f\left(\frac{1}{F}\right)$ by finding the minimum sum of the squares of deviations for points taken from the curve $T = f\left(\frac{1}{F}\right)$ from the approximating linear function depends on the impurity concentration. It is therefore impossible to preassign the correct part of the curve $T = f\left(\frac{1}{F}\right)$ or the number of iterations required to obtain the accurate purity value. The results of direct application of the recommendations given in [4] and [2] are presented in Fig. 5.

The conclusion to be drawn from the above is that since, in the last analysis, information about the sample purity is carried in the form of the melting curve, which is very sensitive to distortions due to thermal resistances and inertial lags, the average uncertainty of the absolute purity measurements by the more efficient methods of Driscoll et al. and Marti under the optimum experimental conditions ($b \leqslant 2$ deg/min, $m \leqslant 3 \cdot 10^{-6}$ kg) is about 30% in the range $\bar{X}_2 = 0.0075$–0.0135; it increases to 50% over the ranges $\bar{X}_2 = 0.0135$–0.0185 and $\bar{X}_2 = 0.005$–0.0075, and at $\bar{X}_2 < 0.005$ and $\bar{X}_2 > 0.00185$ the error becomes impermissibly high.

The above error estimates refer, strictly speaking, only to the phenacetine-benzamide system whose parameters were taken for the calculations. However, a numerical experiment in which the fusion enthalpy was varied in the range $20 \cdot 10^3$–$80 \cdot 10^3$ J/mol, the fusion temperature in the range 320–500 K, and the interaction energy in the range 200–800 J/mol, showed that these estimates remained valid.

Finally, it is necessary to note that in papers [3], [6] and [7] it is recommended to correct the recorded melting curve using the melting curve slope for an indium sample. This means that the curve to be used in further treatment is obtained from the recorded melting curve through the following procedure. Let g^{rec} denote the recorded power at the moment when the programmed temperature equals T_p. Then, the corrected temperature value T^{cor}, which is assumed to correspond to power g^{rec}, is calculated thus:

$$T^{cor} = T_p - R_i g^{rec}$$

where R_i = thermal resistance determined using the indium melting curve. However, it is necessary to bear in mind that, firstly, the conditions of thermal contact between melting indium and a container and those between melting organic

substances and a container are qualitatively different, as has repeatedly been pointed out, for example in [2]. Secondly, even if values of R_S determined in accordance with the recommendations in [13] are used for correction, the gain in accuracy due to the correction does not exceed 10–15%, since the accuracy of the R_S determination does not exceed 35% and because a mere shift in temperature does not fully take into account complex distortions of the melting curve which occur during the recording of melting by DSC.

The overall conclusion is that accuracy estimates in absolute DSC purity determinations of 20% and less, often cited in the literature, should be considered as overstated. A more realistic estimate in the range $\bar{X}_2 = 0.005$–0.02 is 30–50% when the sample mass is less then $3 \cdot 10^{-6}$ kg and the scanning rate is no more then 1–2 deg/min.

References

1 D. L. Sondack, Anal. Chemistry, 44 (1972) 888.
2 E. E. Marti, Thermochim. Acta, 5 (1972) 173.
3 B. G. Cooksey and R. A. Hill, J. Thermal Anal. 10 (1976) 83.
4 G. L. Driscoll. L. N. Duling and F. Magnotta, Anal. Calorimetry, 1 (1968) 271.
5 G. M. Gustin, Thermochim. Acta, 39 (1980) 81.
6 E. F. Palermo and J. Chiu, Thermochim. Acta, 14 (1976) 1.
7 F. F. Joy, J. D. Bonn and A. J. Jr. Barnard, Thermochim. Acta, 2 (1971) 57.
8 Gy. Kiss, K. Seybold and T. Meisel. J. Thermal Anal., 21 (1981) 49.
9 M. Draguet-Bruchmans and R. Bouche, J. Thermal Anal., 20 (1981) 141.
10 C. Plato and A. R. Glasgo, Anal. Chemistry, 41 (1969) 331.
11 Mettler Information TA-2000 No. 1.
12 V. I. Kulagin and A. A. Raskin, "Promishlennaya Teplotechnika", 4 (1982) 95–99 (in Russian).
13 V. I. Kulagin, "Issledovanya v oblasty contaktnoy termometrii i pirometrii izlucheniya", 1982, Energoatomizdat, p. 49–52 (in Russian).
14 A. A. Raskin, Proceedings of the 4 All-Union Symposium "Dynamic measurements", Leningrad, 1984, p. 242–246 (in Russian).
15 U. P. Shlikov, E. A. Ganin and S. A. Tsarevsy, "Contactnie termicheskie soprotivlenia", M., Energia, 1977 (in Russian).

Zusammenfassung — Eine Vergleichende Analyse verschiedener Methoden zur Reinheitsbestimmung mittels DSC wurde ausgeführt. Diese basiert auf einem mathematischen System, daß die Konstruktion theoretischer Schmelzkurven für Zweikomponentensysteme und die Berechnung von registrierten Schmelzkurven mit Hilfe einer Reihe die Ausbildung des DSC-Signals beschreibenden Gleichungen in sich einschließt. Es wird gezeigt, daß die Genauigkeit der Reinheitsbestimmungen bei Konzentrationen der Verunreinigungen von $\bar{X}_2 = 0.005$–0.02 30–50% nicht überschreitet.

Резюме — Проведен сравнительный анализ ряда методов определения степени чистоты с помощью дифференциальных сканирующих калориметров на основе математической модели, включающей построение теоретической кривой плавления двухкомпонентных систем и расчет регистрируемой кривой плавления на основе системы уравнений, описывающей формирование выходного сигнала ДСК. Показано, что точность определений степени чистоты в диапазоне концентрации примеси 0,005–0,02 не превышает 30–50%.